Applied Geochemistry 86 (2017) 84–91

Contents lists available at ScienceDirect

Applied Geochemistry

journal homepage: www.elsevier.com/locate/apgeochem

Diffusion of radiosulphate and radiocaesium in kaolinite clay (KGa-2): Testing the applicability of the pore water diffusion model

David Aldaba [a], Martin A. Glaus [b], Luc R. Van Loon [b], Anna Rigol [a, *], Miquel Vidal [a]

[a] Chemical Engineering and Analytical Chemistry Department, Universitat de Barcelona, 08028 Barcelona, Spain
[b] Laboratory for Waste Management, Paul Scherrer Institut, CH-5232 Villigen, Switzerland

ARTICLE INFO

Article history:
Received 11 April 2017
Received in revised form
14 September 2017
Accepted 25 September 2017
Available online 27 September 2017

Handling editor: S. Stroes-Gascoyne.

Keywords:
Radiocaesium
Radiosulphate
Diffusion
Sorption
Kaolinite

ABSTRACT

The effective diffusion coefficients (D_e) and rock capacity factors (α) for radiosulphate and radiocaesium in compacted kaolinite (KGa-2) were measured as a function of the concentration of $NaClO_4$ in the contacting solution to test the effect of salinity on diffusion of these species. Solid-liquid distribution coefficients (K_d) were derived from α and compared with K_d values from batch sorption experiments using dispersed clay suspensions. D_e values for radiosulphate ($3.3–8.0 \times 10^{-11}$ m^2 s^{-1}) showed no substantial dependence on the concentration of $NaClO_4$. The diffusion K_d values ($9–40$ L kg^{-1}) indicated a weak sorption process, confirmed by the low K_d values measured in the batch sorption experiments. No unambiguous conclusion could be drawn regarding a potential salinity effect on radiocaesium D_e values ($1.4–3.0 \times 10^{-10}$ m^2 s^{-1}). The diffusion-derived K_d of ^{134}Cs ($53–498$ L kg^{-1}) varied inversely with the $NaClO_4$ concentration, consistent with a cation exchange process, and substantially decreased in the presence of stable Cs, suggesting the presence of specific sites for ^{134}Cs that become saturated at high Cs concentrations. Structural analyses indicated an illite content of around 1.7%, which explained the generally large K_d values for radiocaesium. Finally, the correlation between measured D_e values and the respective diffusion coefficients in bulk water (D_w) was examined for a number of species, including radiosulphate and radiocaesium in the presence of stable Cs, along with additional data gathered from other species. Both variables were highly correlated, confirming the validity of the pore water diffusion model, but only in the absence of specific interaction with the clay.

1. Introduction

The deep geological repository (DGR), based on a combination of engineered and natural barriers, is internationally considered to be the safest option for isolating and managing highly radioactive waste (OECD/NEA, 1995). Argillaceous media have been widely proposed as suitable host rocks and backfilling barrier materials for these repositories, because they retard radionuclide migration due to their low hydraulic conductivity and excellent retention capacity for many radionuclides (ANDRA, 2005; NAGRA, 2002). Diffusion and sorption are processes governing the transport of radionuclides in the clays barriers of a DGR. For this reason, an in-depth knowledge of these processes is necessary for the performance assessment of the facility.

The available pathways for solute diffusion in clays depend on the aggregation of tetrahedrally-coordinated silicon (T) and octahedrally-coordinated aluminium (O) layers, mainly resulting in TO or TOT structures in non-swelling (e.g. kaolinite) and swelling clays (e.g. illite, smectites), respectively. They further depend on the isomorphic substitutions of aluminium and silicon by metal cations of lower charge. The resulting permanent negative structural charges need to be compensated by dissolved counter cations. The type, size and bonding of the counter cation also have a strong impact on the swelling properties of the clay (Sposito et al., 1999).

Solute transport in compacted clays depends on the pore water chemical composition and their retention capacity, which is determined by the properties of clay surface and its degree of compaction. The combination of TO and TOT clay layers results in the formation of clay stacks, and the aggregation of clay stacks determines the presence of pore domains containing different types of pore water (Appelo et al., 2010). On the one hand, it results in the presence of macropores, in both swelling and non-swelling clays, which are filled with interparticle water or bulk water, and in which diffusive transport is affected by the geometry of the pore

* Corresponding author.
E-mail address: annarigol@ub.edu (A. Rigol).

https://doi.org/10.1016/j.apgeochem.2017.09.014
0883-2927/

network. In this context, the pore water diffusion model considers that, for a non-reactive porous medium with a certain pore water composition and porosity (ε), the effective diffusion coefficient (D_e) and the molecular diffusion coefficients in bulk water (D_w) of a given solute follow an empirical relationship that depends mainly on a geometric factor (G). This factor depends on the connectivity of the pore network in terms of the geometric constrictivity and tortuosity of the porous media (Boving and Grathwohl, 2001; Aldaba et al., 2014; Jacops et al., 2017). Thus, the diffusive steady-state fluxes in porous media of solutes would be linearly related to their D_w:

$$D_e = \frac{\varepsilon}{G} \times D_w \quad (1)$$

On the other hand, the negatively charged clay surfaces may induce an excess of cations and a deficit of anions near the clay surface. It is generally assumed that pore water in those domains, frequently denoted as diffuse double layer (DDL) water, has different properties that those of the bulk water. Furthermore, the aggregation of TOT layers in swelling clays determines the presence of nanopores filled with a third type of water, interlayer water, showing a physicochemical behaviour comparable to that of the DDL water (Bourg et al., 2006; González-Sánchez et al., 2008; Appelo et al., 2010; Glaus et al., 2010). In contrast to charge compensating cations in the DDL, the chemical behaviour of the cations in the interlayers is characterised by a reduced availability of water for hydration and the presence of overlapping surface potentials. The excess of cations in the DDL and interlayer water relative to their concentration in bulk water causes larger concentration gradients than those in the interparticle water and, thus, diffusion of cations may be enhanced in such situations (Gimmi and Kosakowsky, 2011). Furthermore, the related deficit of anions explains the slower anion diffusion in these domains (Leroy et al., 2006; Van Loon et al., 2007; Jougnot et al., 2009; Appelo et al., 2010), and also a reduced accessible porosity for anions in compacted swelling clays (Muurinen et al., 2004; Van Loon et al., 2007; Appelo et al., 2010). The interaction of charged species with the charged surface may thus have an impact on the diffusive fluxes induced by changes in the local concentration gradients. Such processes require the surface species to be mobile (Gimmi and Kosakowsky, 2011; Glaus et al., 2013). Because D_e values are defined with respect to the concentration gradients in the bulk aqueous phase, the proportionality between D_e and D_w may be different for a charged compared to a non-charged reference tracer (Glaus et al., 2010).

Non-swelling clays, such as kaolinite, have no interlayer water and exhibit a rather low surface charge capacity (González-Sánchez et al., 2008). Solute diffusion in those clays is expected to occur almost exclusively in the interparticle water and the D_e to be solely affected by geometric properties of the pore structure. If the diffusion occurs within the interparticle water, it is expected that variations in the external ionic strength could slightly affect the D_e, due for instance to changes in water viscosity (Glaus et al., 2010). Besides, if solute sorption at the clay surfaces occurs, it may further influence the linear diffusive velocity of these species by retardation (Van Loon et al., 2007; Glaus et al., 2007, 2010; González-Sánchez et al., 2008). In such cases, the breakthrough behaviour is affected, while the proportionality between D_e and D_w is left untouched.

In this paper, the suitability for the pore water diffusion model to describe the diffusion of anionic ($^{35}SO_4$) and cationic (^{134}Cs) radiotracers was tested in kaolinite clay (KGa-2). The diffusion measurements were carried out at varying concentrations of $NaClO_4$, to represent scenarios with varying ionic strengths, using compacted samples of KGa-2. Additionally, the solid-liquid distribution coefficients, derived from diffusion experiments and determined by batch experiments, were used to examine the sorption of the radiotracers in the target kaolinite.

2. Material and methods

2.1. Reagents

Chemically pure reagents ($NaClO_4$ and CsCl) were purchased from Fluka (Buchs, Switzerland) and VWR (Dietikon, Switzerland), respectively. Solutions of $^{35}SO_4$ and ^{134}Cs were purchased from Eckert & Ziegler Isotope Products (Valencia, CA).

2.2. Clay samples

The kaolinite KGa-2 was obtained from the Source Clay Mineral Repository (University of Missouri, Columbia, MO). A purified KGa-2 sample (pKGa-2) was produced from the initial KGa-2 sample through a peptisation treatment, in which the clay impurities were brought into a non-sedimenting form by equilibration with pure water, and subsequently separated (Bradbury and Baeyens, 2009). To achieve this, 15 g of the initial KGa-2 sample and 75 mL of Milli-Q water were mixed inside dialysis bags (Visking #9, cutoff: 12–14 kDa, Medicell, London, UK), which were then closed and immersed in 2 L of Milli-Q water that was replaced every 8 h at least four times.

Differential thermal analyses (DTA), thermo-gravimetric analyses (TGA), X-ray diffraction (XRD) and ^{29}Si MAS NMR analyses were performed to characterize KGa-2 and pKGa-2 samples. DTA and TGA were performed using a Thermal Analysis (TA) (SDT-Q600) instrument. The sample temperature was increased up to 900 °C at a rate of 10 °C min^{-1} in air and in N_2 atmosphere. Powder X-ray diffraction (XRD) patterns, in the region from 3° to 70°, were obtained using a Panalytical X'Pert Pro, equipped with a Cu-K radiation source. Diffractograms were obtained with a step size of 0.02° and a time step of 10 s. Diffraction peaks were analysed using the DIFFRAC^{plus} Evaluation package. Single-pulse (SP) ^{29}Si MAS-NMR spectra were recorded using a Bruker AVANCE SB400 spectrometer equipped with a multinuclear probe. Powdered samples were packed in 4 mm zirconia rotors and spun at 10 kHz. ^{29}Si MAS NMR spectra were acquired at a frequency of 79.49 MHz, using a pulse width of 2.66 μs s ($\pi/2$ pulse length = 7.32 μs) and a delay time of 40 s. The chemical shift values were reported in ppm with respect to tetramethylsilane.

2.3. Diffusion experiments

All experiments were carried out at temperatures of 22 ± 2 °C and under ordinary laboratory atmosphere.

2.3.1. Radiosulphate diffusion experiments

Radiosulphate diffusion in compacted KGa-2 was investigated using the through-diffusion method, which is usually employed with radionuclides with low sorption capacity and subsequent rapid diffusion (Shackelford, 1991). KGa-2 samples were compacted into cylindrical diffusion cells having a cross-sectional area of 5.22 cm^2 to achieve a bulk density of 1.90 ± 0.05 kg L^{-1} and a porosity of 0.26 ± 0.01. Once compacted, the length of the samples in the diffusion cells was 10.7 mm. The samples were kept confined between two porous stainless steel filters, and the diffusion cells were closed by two end-pieces. Each of the end-pieces of the diffusion cell was connected to a liquid reservoir and the solutions circulated using a peristaltic pump. The source solution had a volume of 250 mL, whereas the solution in the target reservoir had a volume of 25 mL. The experimental setup is very similar to the

setup described by Van Loon et al. (2003). A schematic representation is provided in the Supplementary Information (Fig. S1). Each reservoir was filled with a solution with a given $NaClO_4$ concentration (0.1, 0.5 or 1.0 mol L^{-1}) circulating through the end-pieces and along the porous filters to come into contact with the clay in order to saturate the samples. The sample saturation stage lasted for 4 weeks. Subsequently, a known amount of $^{35}SO_4$ solution was added to the source reservoir to achieve an initial activity concentration around 1200 Bq g^{-1} (2.83×10^{-11} mol L^{-1}). The experiments were carried out in duplicate.

The radiosulphate breakthrough curves were obtained by measuring the flux data, J(x,t) (mol m^{-2} s^{-1}), in the target reservoir as a function of time. To this end, at regular time intervals (between 2 and 7 days), the target reservoir with a certain concentration of accumulated radiosulphate was replaced by a new target reservoir containing radiosulphate-free solution, with the corresponding $NaClO_4$ concentration. The accumulated tracer concentration in the target reservoirs was measured in subsamples (5 mL) by liquid scintillation. Simultaneously, the decrease in radiosulphate concentration in the source reservoir was monitored by sampling and measuring 0.1 mL aliquots. The experiments ended after a maximum observation time of ~350 d.

The breakthrough and reservoir depletion curves obtained were employed to simultaneously derive best-fit parameter values for D_e and rock capacity factor (α). All numerical calculations were carried out using the 'Transport of dilute species' interface of the finite-element analysis Comsol Multiphysics® code. A simplified 1D-linear geometry along the cylindrical axis of the filter–clay–filter sandwich was used for that purpose. The fit parameters and their variances at the 5% confidence level were evaluated using a parameter optimization routine (*lsqnonlin*) implemented in Matlab®.

The quantification of α permitted the derivation of values of the solid-liquid distribution (K_d) obtained in diffusion conditions according to the following equation:

$$\alpha = \varepsilon + \rho_{bulk} \times K_d \quad (2)$$

where ε is the porosity and ρ_{bulk} (kg L^{-1}) is the clay bulk dry density.

2.3.2. Radiocaesium diffusion experiments

The diffusion of radiocaesium was examined by means of in-diffusion experiments, which is a suitable method for studying the diffusion of radionuclides with high sorption capacity and slow diffusion in clays (Shackelford, 1991; Yu and Neretnieks, 1997; Van Loon and Eikenberg, 2005). The experimental set-up (illustrated as Fig. S2 in the Supplementary Information), was similar to that of through-diffusion, but here the diffusion cell was in contact with a source reservoir only. The clay samples were compacted into 10 mm diffusion cells to a bulk density of 1.90 ± 0.05 kg L^{-1} and a porosity of 0.28 ± 0.01.

Two experiments were carried out for radiocaesium as a function of the $NaClO_4$ concentration (0.1, 0.5 or 1.0 mol L^{-1}) in the presence and absence of stable caesium (~10^{-5} mol L^{-1}). After sample saturation with the corresponding concentrations of $NaClO_4$ and stable Cs, ^{134}Cs (around 1 MBq L^{-1}) was added to the reservoir solution and the diffusion process started. A depletion curve for the decrease in the radiocaesium concentration in the reservoir solution was obtained by periodically measuring the ^{134}Cs activity in 0.1 mL aliquots (~0.1 mL) during the experiment. The reduction in volume was considered negligible since it was less than 1%. At the end of the diffusion experiment, which lasted for 14 days, the cells were disassembled and the compacted KGa-2 plugs were carefully cut into slices (0.1–0.2 mm) using a razor blade. Diffusion profiles were obtained by plotting the radiocaesium concentration measured in each slice versus their corresponding position in the diffusion cell.

Data treatment was carried out as described for radiosulphate by applying both the 'Transport of dilute species' interface of the finite-element analysis Comsol Multiphysics® and the Matlab® optimization routine. The corresponding K_d values were derived from Eq. (2).

2.4. Sorption experiments

2.4.1. Batch sorption experiments with radiosulphate

K_d values of radiosulphate were determined by batch sorption experiments using dispersed suspensions of KGa-2. Fifteen grams of KGa-2 were placed in dialysis bags with 75 mL of $NaClO_4$ solution of a given concentration (0.1, 0.5 and 1.0 mol L^{-1}). Next, the dialysis bags were immersed in ~1000 mL of $NaClO_4$ solution at the same concentrations. The external solution was replaced four times after at least 8 h and, finally, separated from the dialysis bag and labelled with radiosulphate. pH values in the outer dialysis solutions were around 5. Subsequently aliquots of the inner dialysis compartment containing the clay suspension were mixed with a measured volume of the radiolabelled final outer dialysis solution in a 40 mL centrifugation tube to ensure a liquid/solid ratio of 10 mL/g. The vials were shaken end-over-end at 30 rpm for one week. Next, the phases were separated by centrifugation (98,000 *g*, 30 min), and the activity in the supernatant was measured by liquid scintillation. K_d was quantified as follows:

$$K_d = \frac{A_{in} - A_{eq}}{A_{eq}} \times \frac{V}{m} \quad (3)$$

where A_{in} is the initial radionuclide activity in the contact solution (Bq) (separately determined from aliquots of the outer dialysis solution containing radiosulphate), A_{eq} (Bq) is the final equilibrium radiosulphate activity in the supernatant, V is the volume of solution (L) and m is the dry mass of clay (kg).

2.4.2. Batch sorption experiments with radiocaesium

K_d values of ^{134}Cs were obtained for KGa-2 in the presence of stable caesium. Samples were preequilibrated, as described for radiosulphate, but with a 0.1 mol L^{-1} $NaClO_4$ solution with a known concentration of stable caesium (10^{-8}, 5×10^{-7}, 10^{-7}, 5×10^{-6}, 10^{-6}, 5×10^{-5}, 10^{-5}, 5×10^{-4}, 10^{-4}, 5×10^{-3} and 10^{-3} mol L^{-1}). The liquid/solid ratio for the K_d measurements was 35 mL/g, the rest of the test being as described for radiosulphate.

2.4.3. Determination of K_d (^{134}Cs) at variable NH_4-to-K concentration ratios in contact solutions

Additional batch sorption experiments were carried out both for KGa-2 and pKGa-2 samples under variable concentration ratios of sorption competing species, NH_4 and K. To achieve this, the K_d for radiocaesium was obtained in six scenarios, in which the same concentrations of Ca and K (0.1 and 0.01 mol L^{-1}, respectively) and increasing NH_4 concentrations (0, 0.5, 1.0, 2.5, 4.0 and 5.0 mmol L^{-1}) were applied (Wauters et al., 1996). The clay samples (0.25 g) were pre-equilibrated three times with 25 mL of these solutions, the supernatant being decanted off after each pre-equilibration following centrifugation at 13,000 *g*. Finally, the samples were shaken for 16 h with the same volume of each solution labelled with ^{134}Cs. K_d (^{134}Cs) were derived from the quantification of ^{134}Cs activity concentration in the initial and final solutions.

2.5. Activity measurements

The activity of $^{35}SO_4$ was quantified by liquid scintillation employing a Tri-carb 2250 CA counter (Canberra-Packard) in 1:1 mixtures of sample solution and scintillation cocktail (Ultima Gold XR, Canberra-Packard), using the energy window of 0–45 keV.

Measurements of the ^{134}Cs activity were performed for 12 min by γ-counting (Minaxi-γ, Autogamma 5000 series, Packard) using the energy window of 615–675 keV. All samples were brought to a final volume of 5 ml. The specific ^{134}Cs activity in the clay slices was measured after addition of ~5 mL of 0.1 mol L^{-1} HCl to achieve a homogeneous tracer distribution in the samples. Results were corrected for the humidity content of the clay slices.

All the activity measurements were corrected for the respective radionuclide decay between the measurement and chosen reference dates.

3. Results and discussion

3.1. Diffusion and sorption of $^{35}SO_4$ in KGa-2: role of the external salt concentration

Table 1 summarizes the best-fit parameter values for D_e and α, and the respective relative errors, obtained for the diffusion of radiosulphate in KGa-2 as a function of the external concentration of $NaClO_4$. Table 1 also shows the K_d derived from α values of the diffusion experiments and those obtained from batch sorption experiments. As representative examples, Fig. 1a and b, respectively, show the breakthrough and the depletion curves in the source reservoir for the experiment carried out in the presence of 1.0 mol L^{-1} $NaClO_4$.

The D_e values of radiosulphate ranged from 3.3×10^{-11} to 8.0×10^{-11} m^2 s^{-1}, almost two orders of magnitude lower than the value of the radiosulphate diffusion coefficient in free water (D_w) at 25 °C (1.07×10^{-9} m^2 s^{-1}) published by Li and Gregory (1974). Although the large uncertainty associated with the derived D_e values precludes any unequivocal conclusions, the D_e slightly decreased when the concentration of $NaClO_4$ increased, thus indicating that an increase in salinity could affect the effective diffusion of this radiotracer. If the results are discussed on the basis of the classical pore water diffusion model, the G factor for radiosulphate can be deduced from Eq. (1) and compared to that of non-reactive reference species, for which HTO was chosen in the present work. The G values for HTO were estimated from a D_w value of 2.3×10^{-9} m^2 s^{-1} (Li and Gregory, 1974) and the D_e values obtained in the KGa-2 clay ($1.3–1.7 \times 10^{-10}$ m^2 s^{-1}) by Glaus et al. (2010), and ranged from 3.8 to 5.0. These values were in the same range as those obtained by Jacops et al. (2017) for HTO in Boom Clay. The same calculation for $^{35}SO_4$ resulted in G values between 3.5 and 8.4. Thus, the radiosulphate diffusion process was governed mainly by the connectivity of the pore network at low salinity, but when salinity increases slight discrepancies may be expected in view of the different response of this solute to changes in viscosity of the liquid phase (Glaus et al., 2010).

The pattern of variation of the radiosulphate K_d values with respect to changes in $NaClO_4$ concentration was similar regardless of the methodology used. The individual diffusion and batch K_d values for each $NaClO_4$ concentration were not the same due to the effect of the methodology, as already shown for other radionuclides (Aldaba et al., 2010). Focusing on radiosulphate diffusion K_d, values were generally low, thus confirming a low interaction with the clay, although values tended to decrease slightly with increasing concentrations of $NaClO_4$. A likely explanation for the sorption of these anionic species can be found in the affinity of protonated edge sites of the KGa-2 layers. Note that the pH values measured in the target reservoir during the experiments (between 5.0 and 5.4), could justify the presence of such positive local charges in the KGa-2 in view of the point of zero charge being around 5.5 (Huertas et al., 1998). A minor effect of ClO_4^- competition with radiosulphate for sorption at high $NaClO_4$ concentrations should not be ruled out as being potentially responsible for the minor decrease in radiosulphate K_d when increasing the salinity of the solution.

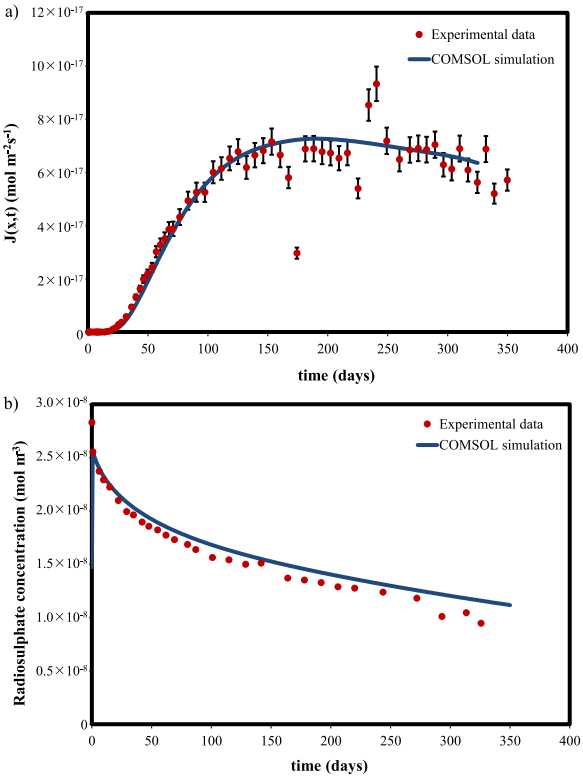

Fig. 1. Radiosulphate diffusion in KGa-2 pre-equilibrated with $NaClO_4$ 1.0 mol L^{-1}. a) Breakthrough curve. b) Depletion curve in the source reservoir during radiosulphate diffusion.

3.2. Diffusion and sorption of ^{134}Cs in KGa-2 samples: role of the external salt concentration and of the presence of stable element

Table 2 shows the best-fit parameter values for D_e, α and K_d derived from the radiocaesium diffusion experiments as a function of the external concentration of $NaClO_4$. All tracer profiles could be satisfyingly modelled using a constant-K_d approach for a given salinity scenario. Representative examples of ^{134}Cs diffusion results (tracer profile in the clay and tracer depletion curve in the source reservoir) are shown in Fig. 2a and b.

D_e values for ^{134}Cs in the absence of stable Cs decreased at the maximum salt concentration assayed. This decrease might be

Table 1
Values of diffusion and sorption parameters obtained for $^{35}SO_4$. Associated errors for all parameters are expressed as one standard deviation (within brackets).

$NaClO_4$ (mol L^{-1})	$D_e \times 10^{-11}$ (m^2 s^{-1})	α	K_d (L kg^{-1}) Diffusion	Batch
0.1	8 (4)	70 (35)	40 (20)	110 (20)
0.5	3.3 (0.3)	18 (2)	9 (4)	30 (6)
1.0	4.5 (0.5)	18 (2)	10 (5)	20 (4)

Table 2
Values of diffusion and sorption parameters obtained for ^{134}Cs in the absence and presence of stable caesium (10^{-5} mol L^{-1}). Associated errors for all parameters are expressed as one standard deviation (within brackets).

$NaClO_4$ (mol L^{-1})	Without stable Cs			With stable Cs		
	$D_e \times 10^{-10}$ (m^2 s^{-1})	α	K_d (L kg^{-1})	$D_e \times 10^{-10}$ (m^2 s^{-1})	α	K_d (L kg^{-1})
0.1	3.0 (1.4)	945 (408)	498 (215)	1.5 (0.5)	63 (22)	33 (12)
0.5	3.0 (1.3)	500 (225)	267 (120)	2.6 (0.6)	20 (5)	11 (3)
1.0	1.4 (0.6)	99 (43)	53 (23)	1.6 (0.5)	12 (2)	5 (1)

explained by changes in water viscosity with the ionic strength, and by potential effects of surface diffusion (Glaus et al., 2010). G values for ^{134}Cs were derived using a D_w of 2.07 × 10^{-9} m^2 s^{-1} (Li and Gregory, 1974) and ranged from 1.9 to 4.1. Although this range overlapped with that of HTO, the G values for ^{134}Cs were generally lower. The low G values in the scenarios with lower Na concentration might be an indication that radiocaesium diffusion is influenced by sorption.

Diffusion-derived K_d values measured in the absence of stable Cs were much higher than the corresponding values measured in the presence of stable Cs, and they decreased with increasing concentration of $NaClO_4$ in both cases. Whereas the high K_d values might indicate that part of the ^{134}Cs sorption could be governed by the presence of specific sites the decrease observed as Na concentration increased may indicate Na competition for ^{134}Cs sorption. For a 1:1 cation exchange process of monovalent cations according to the following reaction

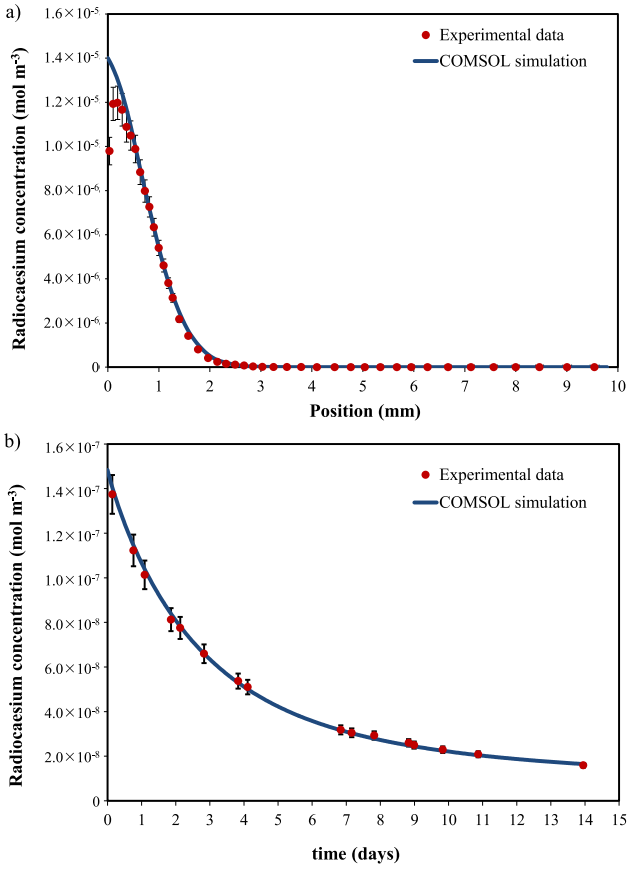

Fig. 2. a) Diffusion profile obtained for radiocaesium (without extra addition of stable Cs) in KGa-2 clay pre-equilibrated with $NaClO_4$ 0.1 mol L^{-1}. b) Depletion curve in the reservoir during radiocaesium diffusion.

$$\text{A-clay} + B^+ = \text{B-clay} + A^+ \quad (4)$$

The B-to-A selectivity coefficient, K_c (B/A), is defined for trace concentrations of B according to the Gaines-Thomas convention as:

$$K_c(B/A) = K_d(B) \times \frac{[A]}{CEC} \times \frac{\gamma_A}{\gamma_B} \quad (5)$$

where CEC is the cation exchange capacity (eq kg^{-1}), [A] the solution concentration of A species (mol L^{-1}) and γ the activity coefficients of cations A and B. Assuming the CEC is of the order of 0.03 eq kg^{-1} and that the activity coefficients for Na and Cs cancel each other out, the K_c (Cs/Na) values derived from the diffusion experiments at trace caesium concentrations would range from ~1700 to ~4500 for the experiments carried out in the absence of added stable Cs. This range is much larger than previously published K_c (Cs/Na) values for regular exchangeable sites in clay (Gast, 1972), which range between 1 and 18.

When diffusion experiments were carried out in the presence of stable caesium the D_e values of ^{134}Cs did not depend on the $NaClO_4$ concentration, with D_e and α values generally lower than those obtained without stable caesium. G values ranged from 2.2 to 3.9, similar to those obtained in the absence of stable caesium. The diffusion-derived K_d values were more than one order of magnitude lower than without stable caesium, and they decreased slightly as Na concentration increased. The K_c (Cs/Na) values were in the range of 110–183, still higher than that expected at regular exchange sites, but also much lower than that quantified in the absence of stable caesium. Therefore, the stable caesium masked the ^{134}Cs sorption at high affinity sites, which may be present in the KGa-2 clay sample.

To confirm the role of stable caesium in the diffusion and sorption of ^{134}Cs, K_d values of ^{134}Cs were also measured in dispersed suspensions of KGa-2 at a constant 0.1 mol L^{-1} $NaClO_4$ concentration and increasing stable Cs concentrations (see Fig. S3 in the Supplementary Information). The low K_d (^{134}Cs) values, similar to those obtained in the diffusion experiments with stable caesium, and the continuous decrease of K_d (^{134}Cs) with increasing concentration of stable caesium suggested that, in the presence of stable Cs, radiocaesium interaction in the KGa-2 samples was governed by regular exchange sites.

Summarising the observations of ^{134}Cs diffusion and batch sorption experiments, sorption sites with high affinity for Cs appear to be present in KGa-2. In the presence of a substantial background concentration of stable Cs these sites were masked, leading to a slight decrease in D_e values, and a significant decrease in α, K_d and Cs/Na selectivity.

3.3. Evidence of the presence of high affinity sites for caesium in KGa-2

With the aim of further confirming the presence of high affinity sites in the KGa-2, additional structural analyses and sorption experiments were carried out.

3.3.1. Structural analyses

Differential thermal analyses (DTA) and thermogravimetric analyses (TGA) indicated the presence of other mineral phases in the KGa-2, inferred from the lower weight loss observed in the initial KGa-2 sample than in the pure kaolinite sample (see further explanations and Fig. S4 in the Supplementary Information).

Regarding XRD analyses, the diffractogram of untreated KGa-2 (Fig. 3) matched with the pattern of kaolinite (PDF 01-089-6538) except for a small reflection marked by an asterisk, which corresponded to illite 2M1 (PDF 00-009-0334). It is quite common to find illite together with kaolinite as the result of diagenetic transformation of kaolinite. Illite is a TOT clay mineral that presents well-known high affinity sites (frayed edge sites, FES) for radiocaesium sorption (Comans et al., 1991).

Finally, the ^{29}Si MAS NMR spectrum of the untreated KGa-2 (Fig. S4b, black line) showed two signals in the range −80 and −100 ppm, which are typical of the Q3 environment of clay minerals. The highest signal was centred at −91.3 ppm and was due to the Q3(0Al) environment of kaolinite, and the small signal at −84.4 ppm (marked by an asterisk) was due to the Q3(1Al) environment, which could be due to illite. The deconvolution of the spectrum confirmed that 1.7% of the total Si atoms corresponded to the illite phase. Although being a minor component, previous sorption studies in soils had shown that minor amounts of this clay may govern radiocaesium sorption (Rigol et al., 1998). Instead, the ^{29}Si MAS NMR spectrum of the purified KGa-2 (Fig. S4b, grey line) showed a unique resonance at −91.3 ppm due to kaolinite.

3.3.2. Radiocaesium sorption studies in mixed Ca-K-NH$_4$ scenarios

The procedure of discriminating between Cs binding to FES sites and regular cation exchange sites relies on the measurement of the response of K_d (^{134}Cs) to increasing NH_4 concentrations in solutions containing fixed K and Ca concentrations (Wauters et al., 1996). At trace conditions under which radiocaesium is associated with FES of the illite, the K_d for Cs in KGa-2 would be expected to be sensitive to changes in NH_4 and K concentrations, because these cations also have high affinities for FES, although NH_4 is more competitive than K for these sites, with trace NH_4-to-K selectivity coefficients higher than 1 (Sweeck et al., 1990). On the contrary, if radiocesium is interacting with regular sorption sites, such as those of TO clays like kaolinite, K_d would not change with NH_4 concentration, since NH_4 and K at these sites are equally competitive, and cationic exchange would be controlled by the large Ca concentration (Bruggenwert and Kamphorst, 1982; Cremers et al., 1990).

If FES exist, it can be shown that the ratio of radiocaesium K_d quantified in the presence and absence of NH_4 can be expressed as a function of the NH_4-to-K selectivity coefficient in FES, $K_c(NH_4/K)$ (Wauters et al., 1996):

$$\frac{K_d(Ca-K)}{K_d(Ca-K-NH_4)} = 1 + K_c(NH_4/K) \times \frac{m_{NH_4}}{m_K} \quad (6)$$

where m_K and m_{NH4} are the concentrations of K and NH_4 in mmol L^{-1}, K_d (Ca-K) is the sorption distribution coefficient of ^{134}Cs measured in the absence of NH_4 at given concentrations of Ca and K, while K_d (Ca-K-NH_4) is the sorption distribution coefficient measured in the same conditions, but with varying concentrations of NH_4. Instead, in the absence of FES, this ratio tends to one. Thus, the slope in a representation of K_d (Ca-K)/K_d(Ca-K-NH_4) as a function of the m_{NH4}/m_K concentration ratio reveals directly whether Cs is bound to FES or to less specific cation exchange sites.

Results from the sorption experiments indicated that the K_d (^{134}Cs) in the KGa-2 sample ranged from 16.1 to 6.7 L kg^{-1} as NH_4 concentration increased, whereas the K_d (^{134}Cs) values for the purified pKGa-2 clay sample were virtually constant, with values around 11 L kg^{-1}. As shown in Fig. 4, the response of the K_d (^{134}Cs)

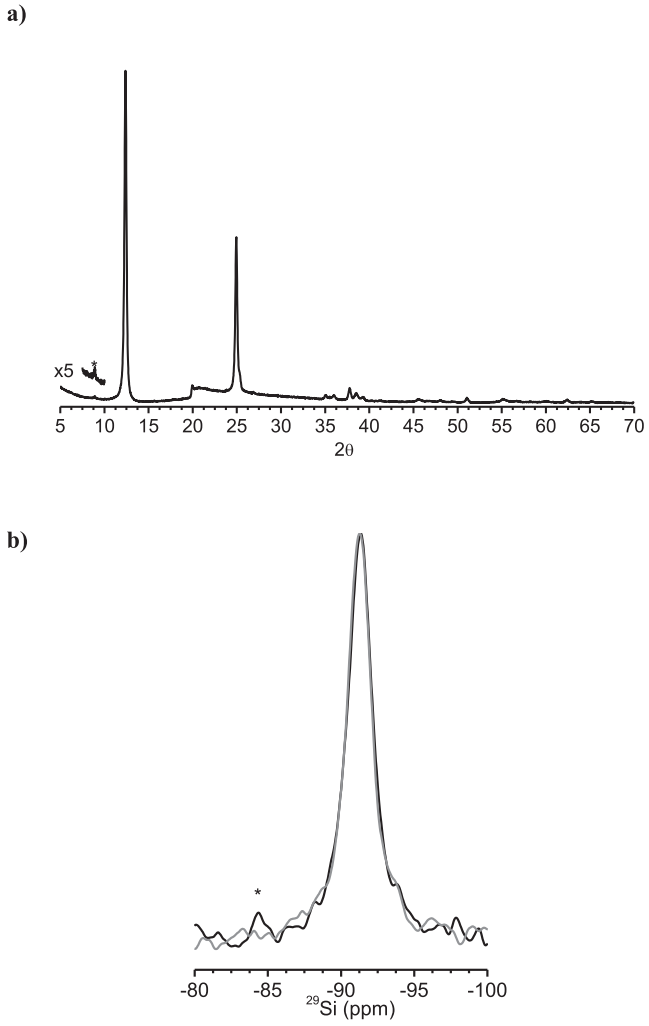

Fig. 3. a) XRD of KGa-2 and detail of the *060* reflection. b) ^{29}Si MAS NMR spectra of KGa-2: untreated (black line) and purified (grey line).

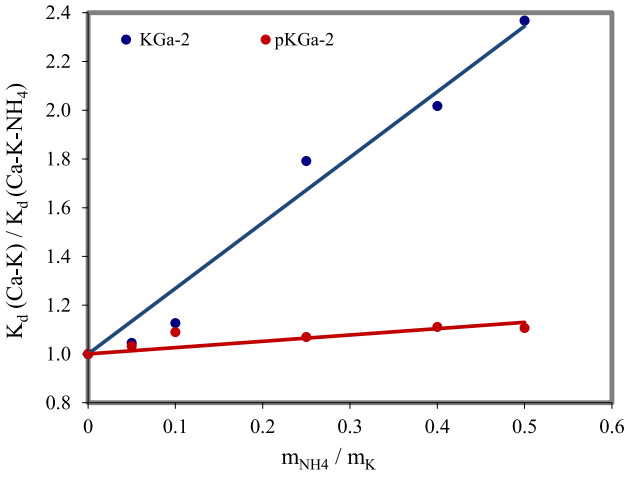

Fig. 4. Response of radiocaesium solid-liquid distribution coefficient (K_d) to increasing NH_4 concentrations in KGa-2 and pKGa-2 samples.

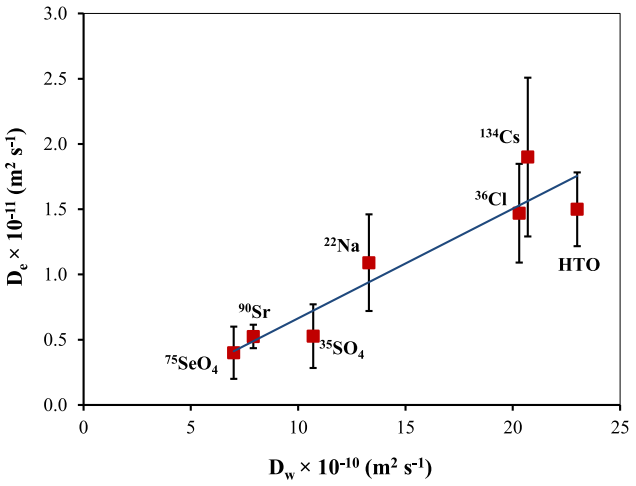

Fig. 5. Relationship between D_e and D_w values in KGa-2 clay for a set of radionuclides. Black line denotes correlation of all solutes.

to increasing NH_4 concentrations confirmed the presence of FES in the KGa-2 with a K_c (NH_4/K) value of 2.8, whereas such a pattern was not observed for the pKGa-2. Therefore, these results indicated that despite the low amount of illite present in the KGa-2, this minor phase had a significant effect on the radiocaesium sorption, possibly enhanced by the compaction of the samples.

3.4. Evaluation of the diffusion results by the classical pore water diffusion model

As concluded from the previous sections, diffusion of $^{35}SO_4$ in KGa-2 is controlled mainly by the interparticle pore connectivity, with a minor effect of salinity at the maximum concentration of $NaClO_4$ tested. The same behaviour was observed for ^{134}Cs in the presence of stable Cs, while an additional contribution of surface bound species may substantially influence the measured D_e values of ^{134}Cs in the absence of stable Cs. Therefore, to evaluate the applicability of the classical pore water diffusion model, by applying Eq. (1), only the D_e values of ^{134}Cs in the presence of stable Cs were taken into account. The $^{35}SO_4$ and ^{134}Cs data were correlated with reported D_e and D_w values of ^{22}Na, ^{36}Cl and HTO (Li and Gregory, 1974; Glaus et al., 2010) and ^{90}Sr and $^{75}SeO_4$ data (personal communication from Glaus). For every radionuclide, in view of the minor effects of the external salt concentration on diffusion, an averaged value of D_e (from 0.1 to 1.0 mol L^{-1} $NaClO_4$) was employed in the correlation. Fig. 5 shows the results of the correlation exercise. The good linear proportionality obtained (D_e = 0.08 (0.01) × D_w, R^2 = 0.88) indicates that diffusive transport of all species occurs through the interparticle porosity of KGa-2 when no specific interaction processes with the clay surface take place.

4. Conclusions

The classic pore water diffusion model, in which the effective diffusion coefficients are only influenced by geometric effects, appropriately describes the diffusive behaviour of radiosulphate and radiocaesium (with a background of stable Cs) in KGa-2, as previously observed for other species. Changes in the ionic strength of the contact solution did not substantially affect either D_e values or the applicability of the model.

Thus, the linear correlation between D_e and D_w values may be applicable for approximate predictions of radionuclide behaviour in an ideally pure kaolinite. However, discrepancies from such a simple approach might be observed if additional driving forces for diffusion, different from the gradient of the bulk aqueous species, occur. This is the case for radiocaesium, where deviations from such an ideal behaviour are caused by very small impurities of illite in the raw KGa-2 material used.

Acknowledgments

This research was funded by the Spanish Government (CICYT, contracts CTM2011-27211 and CTM2014-55191-R) and the Generalitat de Catalunya (AGAUR 2014SGR1277). The authors would like to thank the Paul Scherrer Institut and Nagra for the material support for this research. Dr. M.D. Alba is acknowledged for her help in the DTA, TGA, XRD and NMR analyses as well as in the interpretation of the results. Analyses were performed at the Textural and Thermal Analysis Service, the X-ray Diffraction Service and the Spectroscopy Service of the ICMS (CSIC-US, Seville, Spain).

Appendix A. Supplementary data

Supplementary data related to this article can be found at https://doi.org/10.1016/j.apgeochem.2017.09.014.

References

Aldaba, D., Fernández-Torrent, R., Rauret, G., Vidal, M., Rigol, A., 2010. Laboratory experiments to characterize radiochloride diffusion in unsaturated soils. Appl. Radiat. Isot. 68, 393–398.
Aldaba, D., Glaus, M.A., Leupin, O., Van Loon, L.R., Vidal, M., Rigol, A., 2014. Suitability of various materials for porous filters in diffusion experiments. Radiochim. Acta 102, 723–730.
ANDRA, 2005. Dossier 2005 Argile. Evaluation of the Feasibility of a Geological Repository in an Argillaceous Formation (Synthesis Report, Andra, Paris, France).
Appelo, C.A.J., Van Loon, L.R., Wersin, P., 2010. Multicomponent diffusion of a suite of tracers (HTO, Cl, Br, I, Na, Sr, Cs) in a single sample of opalinus clay. Geochim. Cosmochim. Ac 74, 1201–1219.
Bourg, I.C., Sposito, G., Bourg, A.C.M., 2006. Tracer diffusion in compacted, water-saturated bentonite. Clay Clay Min. 54, 363–374.
Boving, T.B., Grathwohl, P., 2001. Tracer diffusion coefficients in sedimentary rocks: correlation to porosity and hydraulic conductivity. J. Contam. Hydrol. 53, 85–100.
Bradbury, M.H., Baeyens, B., 2009. Sorption modelling on illite Part I: titration measurements and the sorption of Ni, Co, Eu and Sn. Geochim. Cosmochim. Ac 73, 990–1003.
Bruggenwert, M.G.M., Kamphorst, A., 1982. Survey of experimental information on cation exchange in soil systems. In: Bolt, G.H. (Ed.), Soil Chemistry, B. Physicochemical Models. Elsevier, Amsterdam, pp. 141–203 (Chapter 5).
Comans, R.N.J., Haller, M., de Preter, P., 1991. Sorptium of cesium on illite: non-equilibrium behavior and reversibility. Geochim. Cosmochim. Ac 53, 433–440.
Cremers, A., Elsen, A., Valke, E., Wauters, J., Sandalls, F.J., Gaudern, S.L., 1990. The sensitivity of upland soils to radiocesium contamination. In: Desmet, G., Nassimbeni, P., Belli, M. (Eds.), Transfer of Radionuclides in Natural and Semi-natural Environments. Elsevier Applied Science, London, pp. 238–248. EUR 12448.
Gast, R.G., 1972. Alkali-metal cation-exchange on chambers montmorillonite. Soil Sci. Soc. Am. Pro 36, 14–19.
Gimmi, T., Kosakowsky, G., 2011. How mobile are sorbed cations in clays and clay rocks? Environ. Sci. Technol. 45, 1443–1449.
Glaus, M.A., Baeyens, B., Bradbury, M.H., Jakob, A., Van Loon, L.R., Yaroshchuk, A.E., 2007. Diffusion of Na-22 and Sr-85 in montmorillonite: evidence of interlayer diffusion being the dominant pathway at high compaction. Environ. Sci. Technol. 41 (2), 478–485.
Glaus, M.A., Frick, S., Rossé, R., Van Loon, L.R., 2010. Comparative study of tracer diffusion of HTO, $^{22}Na^+$ and $^{36}Cl^-$ in compacted kaolinite, illite and montmorillonite. Geochim. Cosmochim. Ac 74, 1999–2010.
Glaus, M.A., Birgersson, M., Karnland, O., Van Loon, L.R., 2013. Seeming steady-state uphill diffusion of $^{22}Na^+$ in compacted montmorillonite. Environ. Sci. Technol. 47, 11522–11527.
González-Sánchez, F., Van Loon, L., Gimmi, T., Jakob, A., Glaus, M.A., Diamond, L.W., 2008. Self-diffusion of water and its dependence on temperature and ionic strength in highly compacted montmorillonite, illite and kaolinite. Appl. Geochem 23 (12), 3840–3851.
Huertas, F.J., Chou, L., Wollast, R., 1998. Mechanism of kaolinite dissolution at room temperature and pressure: Part I. surface speciation. Geochim. Cosmochim. Ac 62, 417–431.
Jacops, E., Aertsens, M., Maes, N., Bruggeman, C., Krooss, B.M., Amann-

Hildenbrand, A., Swennen, R., Littke, R., 2017. Interplay of molecular size and pore network geometry on the diffusion of dissolved gases and HTO in Boom Clay. Appl. Geochem 76, 182–195.
Jougnot, D., Revil, A., Leroy, P., 2009. Diffusion of ionic tracers in the Callovo-Oxfordian clay-rock using the Donnan equilibrium model and the formation factor. Geochim. Cosmochim. Ac 73, 2712–2726.
Leroy, P., Revil, A., Coelho, D., 2006. Diffusion of ionic species in bentonite. J. Colloid Interf. Sci. 296, 248–255.
Li, Y.-H., Gregory, S., 1974. Diffusion of anions in seawater and in deep-sea sediments. Geochim. Cosmochim. Ac 88, 703–714.
Muurinen, A., Karnland, O., Lehikoinen, J., 2004. Ion concentration caused by a external solution into the pore water of compacted bentonite. Phys. Ch. Ear 29, 119–127.
NAGRA, 2002. Project Opalinus Clay: Safety Report. Demonstration of Disposal Feasibility for Spent Fuel, Vitrified High-level Waste and Long-lived Intermediate-level Waste (Entsorgungsnachweis). Nagra Technical Report NTB-02–05 (Nagra, Wettingen, Switzerland).
OECD/NEA, 1995. The Environmental and Ethical Basis of Geological Disposal of Long-lived Radioactive Wastes. A Collective Opinion of the Radioactive Waste Management Committee of the OECD Nuclear Energy Agency, OECD, Paris.
Rigol, A., Vidal, M., Rauret, G., Shand, C.A., Cheshire, M.V., 1998. Competition of organic and mineral phases in radiocaesium partitioning in organic soils of Scotland and the area near Chernobyl. Environ. Sci. Technol. 32 (5), 663–669.
Shackelford, C.D., 1991. Laboratory diffusion testing for waste disposal – a review. J. Contam. Hydrol. 7, 177–217.
Sposito, G., Skipper, N.T., Sutton, R., Park, S.H., Soper, A.K., Greathouse, J.A., 1999. Surface geochemistry of the clay minerals. P. Natl. Acad. Sci. U. S. A. 96, 3358–3364.
Sweeck, L., Wauters, J., Valcke, E., Cremers, A., 1990. The specific interception potential of soils for radiocaesium. In: Desmet, G., Nassimbeni, P., Belli, M. (Eds.), Transfer of Radionuclides in Natural and Seminatural Environments. Elsevier Applied Science, London, pp. 249–258. EUR 12448.
Van Loon, L.R., Soler, J.M., Jakob, A., Bradbury, M.H., 2003. Effect of confining pressure on the diffusion of HTO, $^{36}Cl^-$ and $^{125}I^-$ in a layered argillaceous rock (opalinus clay): diffusion perpendicular to the fabric. Appl. Geochem 18, 1653–1662.
Van Loon, L.R., Eikenberg, J., 2005. A high-resolution abrasive method for determining diffusion profiles of sorbing radionuclides in dense argillaceous rocks. Appl. Radiat. Isot. 63 (1), 11–21.
Van Loon, L.R., Glaus, M.A., Müller, W., 2007. Anion exclusion effects in compacted bentonites: towards a better understanding of anion diffusion. Appl. Geochem 22, 2536–2552.
Wauters, J., Vidal, M., Elsen, A., Cremers, A., 1996. Prediction of solid/liquid distribution coefficients of radiocaesium in soils and sediments. Part two: a new procedure for solid phase speciation of radiocaesium. Appl. Geochem 11, 595–599.
Yu, J.W., Neretnieks, I., 1997. Diffusion and Sorption Properties of Radionuclides in Compacted Bentonite. SKB Technical Report TR-97–12. Swedish Nuclear Fuel and Waste Management Co., SKB, Stockholm, Sweden.